

## Angular distributions of leptons from $J/\psi$ 's produced in 920 GeV fixed-target proton-nucleus collisions

I. Abt<sup>24</sup>, M. Adams<sup>11</sup>, M. Agari<sup>14</sup>, H. Albrecht<sup>13</sup>, A. Aleksandrov<sup>30</sup>, V. Amaral<sup>9</sup>, A. Amorim<sup>9</sup>, S. J. Aplin<sup>13</sup>, V. Aushev<sup>17</sup>, Y. Bagaturia<sup>13,37</sup>, V. Balagura<sup>23</sup>, M. Bargiotti<sup>6</sup>, O. Barsukova<sup>12</sup>, J. Bastos<sup>9</sup>, J. Batista<sup>9</sup>, C. Bauer<sup>14</sup>, Th. S. Bauer<sup>1</sup>, A. Belkov<sup>12†</sup>, Ar. Belkov<sup>12</sup>, I. Belotelov<sup>12</sup>, A. Bertin<sup>6</sup>, B. Bobchenko<sup>23</sup>, M. Böcker<sup>27</sup>, A. Bogatyrev<sup>23</sup>, G. Bohm<sup>30</sup>, M. Bräuer<sup>14</sup>, M. Bruinsma<sup>29,1</sup>, M. Bruschi<sup>6</sup>, P. Buchholz<sup>27</sup>, T. Buran<sup>25</sup>, J. Carvalho<sup>9</sup>, P. Conde<sup>2,13</sup>, C. Cruse<sup>11</sup>, M. Dam<sup>10</sup>, K. M. Danielsen<sup>25</sup>, M. Danilov<sup>23</sup>, S. De Castro<sup>6</sup>, H. Deppe<sup>15</sup>, X. Dong<sup>3</sup>, H. B. Dreis<sup>15</sup>, V. Egorytchev<sup>13</sup>, K. Ehret<sup>11</sup>, F. Eisele<sup>15</sup>, D. Emeliyanov<sup>13</sup>, S. Essenov<sup>23</sup>, L. Fabbri<sup>6</sup>, P. Faccioli<sup>6</sup>, M. Feuerstack-Raible<sup>15</sup>, J. Flammer<sup>13</sup>, B. Fominykh<sup>23†</sup>, M. Funcke<sup>11</sup>, Ll. Garrido<sup>2</sup>, A. Gellrich<sup>30</sup>, B. Giacobbe<sup>6</sup>, J. Gläß<sup>21</sup>, D. Goloubkov<sup>13,34</sup>, Y. Golubkov<sup>13,35</sup>, A. Golutvin<sup>23</sup>, I. Golutvin<sup>12</sup>, I. Gorbounov<sup>13,27</sup>, A. Gorišek<sup>18</sup>, O. Gouchtchine<sup>23</sup>, D. C. Goulart<sup>8</sup>, S. Gradl<sup>15</sup>, W. Gradl<sup>15</sup>, F. Grimaldi<sup>6</sup>, J. Groth-Jensen<sup>10</sup>, Yu. Gulitsky<sup>23,36</sup>, J. D. Hansen<sup>10</sup>, J. M. Hernández<sup>30</sup>, W. Hofmann<sup>14</sup>, M. Hohlmann<sup>13</sup>, T. Hott<sup>15</sup>, W. Hulsbergen<sup>1</sup>, U. Husemann<sup>27</sup>, O. Igonkina<sup>23</sup>, M. Ispiryan<sup>16</sup>, T. Jagla<sup>14</sup>, C. Jiang<sup>3</sup>, H. Kapitza<sup>13,11</sup>, S. Karabekyan<sup>26</sup>, N. Karpenko<sup>12</sup>, S. Keller<sup>27</sup>, J. Kessler<sup>15</sup>, F. Khasanov<sup>23</sup>, Yu. Kiryushin<sup>12</sup>, I. Kisel<sup>24</sup>, E. Klinkby<sup>10</sup>, K. T. Knöpfle<sup>14</sup>, H. Kolanoski<sup>5</sup>, S. Korpar<sup>22,18</sup>, C. Krauss<sup>15</sup>, P. Kreuzer<sup>13,20</sup>, P. Križan<sup>19,18</sup>, D. Krücker<sup>5</sup>, S. Kupper<sup>18</sup>, T. Kvaratskheliia<sup>23</sup>, A. Lanyov<sup>12</sup>, K. Lau<sup>16</sup>, B. Lewendel<sup>13</sup>, T. Lohse<sup>5</sup>, B. Lomonosov<sup>13,33</sup>, R. Männer<sup>21</sup>, R. Mankel<sup>30</sup>, S. Masciocchi<sup>13</sup>, I. Massa<sup>6</sup>, I. Matchikhilian<sup>23</sup>, G. Medin<sup>5</sup>, M. Medinnis<sup>13</sup>, M. Mevius<sup>13</sup>, A. Michetti<sup>13</sup>, Yu. Mikhailov<sup>23,36</sup>, R. Mizuk<sup>23</sup>, R. Muresan<sup>10</sup>, M. zur Nedden<sup>5</sup>, M. Negodaev<sup>13,33</sup>, M. Nörenberg<sup>13</sup>, S. Nowak<sup>30</sup>, M. T. Núñez Pardo de Vera<sup>13</sup>, M. Ouchrif<sup>29,1</sup>, F. Ould-Saada<sup>25</sup>, C. Padilla<sup>13</sup>, D. Peralta<sup>2</sup>, R. Pernack<sup>26</sup>, R. Pestotnik<sup>18</sup>, B. AA. Petersen<sup>10</sup>, M. Piccinini<sup>6</sup>, M. A. Pleier<sup>14</sup>, M. Poli<sup>6,32</sup>, V. Popov<sup>23</sup>, D. Pose<sup>12,15</sup>, S. Prystupa<sup>17</sup>, V. Pugatch<sup>17</sup>, Y. Pylypchenko<sup>25</sup>, J. Pyrlik<sup>16</sup>, K. Reeves<sup>14</sup>, D. Reßing<sup>13</sup>, H. Rick<sup>15</sup>, I. Riu<sup>13</sup>, P. Robmann<sup>31</sup>, I. Rostovtseva<sup>23</sup>, V. Rybnikov<sup>13</sup>, F. Sánchez<sup>14</sup>, A. Sbrizzi<sup>1</sup>, M. Schmelling<sup>14</sup>, B. Schmidt<sup>13</sup>, A. Schreiner<sup>30</sup>, H. Schröder<sup>26</sup>, U. Schwanke<sup>30</sup>, A. J. Schwartz<sup>8</sup>, A. S. Schwarz<sup>13</sup>, B. Schwenninger<sup>11</sup>, B. Schwingenheuer<sup>14</sup>, F. Sciacca<sup>14</sup>, N. Semprini-Cesari<sup>6</sup>, S. Shuvalov<sup>23,5</sup>, L. Silva<sup>9</sup>, L. Sözüer<sup>13</sup>, S. Solunin<sup>12</sup>, A. Somov<sup>13</sup>, S. Somov<sup>13,34</sup>, J. Spengler<sup>13</sup>, R. Spighi<sup>6</sup>, A. Spiridonov<sup>30,23</sup>, A. Stanovnik<sup>19,18</sup>, M. Starič<sup>18</sup>, C. Stegmann<sup>5</sup>, H. S. Subramania<sup>16</sup>, M. Symalla<sup>13,11</sup>, I. Tikhomirov<sup>23</sup>, M. Titov<sup>23</sup>, I. Tsakov<sup>28</sup>, U. Uwer<sup>15</sup>, C. van Eldik<sup>13,11</sup>, Yu. Vassiliev<sup>17</sup>, M. Villa<sup>6</sup>, A. Vitale<sup>6,7†</sup>, I. Vukotic<sup>5,30</sup>, H. Wahlberg<sup>29</sup>, A. H. Walenta<sup>27</sup>, M. Walter<sup>30</sup>, J. J. Wang<sup>4</sup>, D. Wegener<sup>11</sup>, U. Werthenbach<sup>27</sup>, H. Wolters<sup>9</sup>, R. Wurth<sup>13</sup>, A. Wurz<sup>21</sup>, S. Xella-Hansen<sup>10</sup>, Yu. Zaitsev<sup>23</sup>, M. Zavertyaev<sup>13,14,33</sup>, T. Zeuner<sup>13,27</sup>, A. Zhelezov<sup>23</sup>, Z. Zheng<sup>3</sup>, R. Zimmermann<sup>26</sup>, T. Živko<sup>18</sup>, and A. Zoccoli<sup>6</sup>

<sup>1</sup> NIKHEF, 1009 DB Amsterdam, The Netherlands <sup>a</sup>

<sup>2</sup> Department ECM, Faculty of Physics, University of Barcelona, E-08028 Barcelona, Spain <sup>b</sup>

<sup>3</sup> Institute for High Energy Physics, Beijing 100039, P.R. China

<sup>4</sup> Institute of Engineering Physics, Tsinghua University, Beijing 100084, P.R. China

<sup>5</sup> Institut für Physik, Humboldt-Universität zu Berlin, D-12489 Berlin, Germany <sup>c,d</sup>

<sup>6</sup> Dipartimento di Fisica dell' Università di Bologna and INFN Sezione di Bologna, I-40126 Bologna, Italy

<sup>7</sup> also from Fondazione Giuseppe Occhialini, I-61034 Fossombrone (Pesaro Urbino), Italy

<sup>8</sup> Department of Physics, University of Cincinnati, Cincinnati, Ohio 45221, USA <sup>e</sup>

<sup>9</sup> LIP Coimbra, P-3004-516 Coimbra, Portugal <sup>f</sup>

<sup>10</sup> Niels Bohr Institutet, DK 2100 Copenhagen, Denmark <sup>g</sup>

<sup>11</sup> Institut für Physik, Universität Dortmund, D-44221 Dortmund, Germany <sup>d</sup>

<sup>12</sup> Joint Institute for Nuclear Research Dubna, 141980 Dubna, Moscow region, Russia

<sup>13</sup> DESY, D-22603 Hamburg, Germany

<sup>14</sup> Max-Planck-Institut für Kernphysik, D-69117 Heidelberg, Germany <sup>d</sup>

<sup>15</sup> Physikalisches Institut, Universität Heidelberg, D-69120 Heidelberg, Germany <sup>d</sup>

<sup>16</sup> Department of Physics, University of Houston, Houston, TX 77204, USA <sup>e</sup>

<sup>17</sup> Institute for Nuclear Research, Ukrainian Academy of Science, 03680 Kiev, Ukraine <sup>h</sup>

<sup>18</sup> J. Stefan Institute, 1001 Ljubljana, Slovenia <sup>i</sup>

<sup>19</sup> University of Ljubljana, 1001 Ljubljana, Slovenia

<sup>20</sup> University of California, Los Angeles, CA 90024, USA <sup>j</sup>

<sup>21</sup> Lehrstuhl für Informatik V, Universität Mannheim, D-68131 Mannheim, Germany

<sup>22</sup> University of Maribor, 2000 Maribor, Slovenia

- <sup>23</sup> Institute of Theoretical and Experimental Physics, 117218 Moscow, Russia <sup>k</sup>  
<sup>24</sup> Max-Planck-Institut für Physik, Werner-Heisenberg-Institut, D-80805 München, Germany <sup>d</sup>  
<sup>25</sup> Dept. of Physics, University of Oslo, N-0316 Oslo, Norway <sup>l</sup>  
<sup>26</sup> Fachbereich Physik, Universität Rostock, D-18051 Rostock, Germany <sup>d</sup>  
<sup>27</sup> Fachbereich Physik, Universität Siegen, D-57068 Siegen, Germany <sup>d</sup>  
<sup>28</sup> Institute for Nuclear Research, INRNE-BAS, Sofia, Bulgaria  
<sup>29</sup> Universiteit Utrecht/NIKHEF, 3584 CB Utrecht, The Netherlands <sup>a</sup>  
<sup>30</sup> DESY, D-15738 Zeuthen, Germany  
<sup>31</sup> Physik-Institut, Universität Zürich, CH-8057 Zürich, Switzerland <sup>m</sup>  
<sup>32</sup> visitor from Dipartimento di Energetica dell' Università di Firenze and INFN Sezione di Bologna, Italy  
<sup>33</sup> visitor from P.N. Lebedev Physical Institute, 117924 Moscow B-333, Russia  
<sup>34</sup> visitor from Moscow Physical Engineering Institute, 115409 Moscow, Russia  
<sup>35</sup> visitor from Moscow State University, 119992 Moscow, Russia  
<sup>36</sup> visitor from Institute for High Energy Physics, Protvino, Russia  
<sup>37</sup> visitor from High Energy Physics Institute, 380086 Tbilisi, Georgia

† *deceased*

<sup>a</sup> supported by the Foundation for Fundamental Research on Matter (FOM), 3502 GA Utrecht, The Netherlands

<sup>b</sup> supported by the CICYT contract AEN99-0483

<sup>c</sup> supported by the German Research Foundation, Graduate College GRK 271/3

<sup>d</sup> supported by the Bundesministerium für Bildung und Forschung, FRG, under contract numbers 05-7BU35I, 05-7DO55P, 05-HB1HRA, 05-HB1KHA, 05-HB1PEA, 05-HB1PSA, 05-HB1VHA, 05-HB9HRA, 05-7HD15I, 05-7MP25I, 05-7SI75I

<sup>e</sup> supported by the U.S. Department of Energy (DOE)

<sup>f</sup> supported by the Portuguese Fundação para a Ciência e Tecnologia under the program POCTI

<sup>g</sup> supported by the Danish Natural Science Research Council

<sup>h</sup> supported by the National Academy of Science and the Ministry of Education and Science of Ukraine

<sup>i</sup> supported by the Ministry of Education, Science and Sport of the Republic of Slovenia under contracts number P1-135 and J1-6584-0106

<sup>j</sup> supported by the U.S. National Science Foundation Grant PHY-9986703

<sup>k</sup> supported by the Russian Ministry of Education and Science, grant SS-1722.2003.2, and the BMBF via the Max Planck Research Award

<sup>l</sup> supported by the Norwegian Research Council

<sup>m</sup> supported by the Swiss National Science Foundation

*Many thanks to Antonio Vitale (1943-2008)*

Received: date / Revised version: date

**Abstract.** A study of the angular distributions of leptons from decays of  $J/\psi$ 's produced in p-C and p-W collisions at  $\sqrt{s} = 41.6$  GeV has been performed in the  $J/\psi$  Feynman- $x$  region  $-0.34 < x_F < 0.14$  and for  $J/\psi$  transverse momenta up to 5.4 GeV/c. The data were collected by the HERA-B experiment at the HERA proton ring of the DESY laboratory. The results, based on a clean selection of  $2.3 \cdot 10^5$   $J/\psi$ 's reconstructed in both the  $e^+e^-$  and  $\mu^+\mu^-$  decay channels, indicate that  $J/\psi$ 's are produced polarized. The magnitude of the effect is maximal at low  $p_T$ . For  $p_T > 1$  GeV/c a significant dependence on the reference frame is found: the polar anisotropy is more pronounced in the Collins-Soper frame and almost vanishes in the helicity frame, where, instead, a significant azimuthal anisotropy arises.

## 1 Introduction

This paper presents a new measurement of the angular distribution of leptons from  $J/\psi$ 's produced inclusively in proton-nucleus collisions at centre-of-mass energy  $\sqrt{s} = 41.6$  GeV. The data were collected by the DESY experiment HERA-B and covered the kinematic ranges  $-0.34 < x_F < 0.14$  in the Feynman- $x$  variable and  $0 < p_T < 5.4$  GeV/ $c$  in transverse momentum. In this domain, the average fraction of  $J/\psi$  mesons coming from  $\chi_c$  and  $\psi'$  decays has been determined as  $\sim 27\%$  [1,2]. Most previous analyses were based on the choice of one specific definition of the polarization frame and were limited to the

measurement of the polar angle distribution, from which the so-called “polarization” parameter is extracted. The present measurement includes for the first time a systematic comparison of the results obtained for the *full* decay angular distribution in three different reference frames – and significant differences are found between them. Some of the results are presented separately for the two target materials used in the experiment (carbon,  $A = 12$ , and tungsten,  $A = 184$ ), leaving open the possibility that the nuclear medium may affect the observed decay kinematics (for example as a consequence of a varying mixture of  $J/\psi$ 's from decays of heavier charmonium states and direct  $J/\psi$ 's). The analysis is based on almost the same

sample used in the measurement of the  $J/\psi$  kinematic distributions described in [3], with a total of about 83000 and 143000  $J/\psi$ 's reconstructed, respectively, in the dimuon and dielectron decay channels (excluding only the small fraction of data collected with titanium). The reader is referred to that paper for a description of detector, data taking, trigger, selection criteria and Monte Carlo simulation.

The next section explains the definitions and conventions used in the measurement (Sect. 2). The results are presented in Sect. 3 and discussed in the conclusions (Sect. 4).

## 2 Definitions

In any chosen reference system, the most general (parity conserving) form of the two-lepton decay angular distribution of a  $J/\psi$  is

$$\frac{dN}{d(\cos\theta)d\phi} \propto 1 + \lambda_\theta \cos^2\theta + \lambda_\phi \sin^2\theta \cos(2\phi) + \lambda_{\theta\phi} \sin(2\theta) \cos\phi, \quad (1)$$

where  $\theta$  is the angle between the direction of the positive lepton and a chosen polarization axis in the  $J/\psi$  rest frame.  $\phi$ , the corresponding azimuthal angle, is defined with respect to the plane of the colliding hadrons;  $\lambda_\theta$ ,  $\lambda_{\theta\phi}$  and  $\lambda_\phi$  are the quantities to be measured.<sup>1</sup> The parameter  $\lambda_\theta$  is usually called ‘‘polarization’’; more generally, any observed deviation of at least one of the three parameters from zero would be the indication of polarized  $J/\psi$  production. Non-zero values of  $\lambda_\phi$  and  $\lambda_{\theta\phi}$  indicate an azimuthal anisotropy of the distribution, which may arise as a consequence of specific choices of the reference frame.

The following different definitions of the polarization axis are commonly used in the literature:

- the direction of the beam momentum (as seen in the  $J/\psi$  rest frame) in the so-called Gottfried-Jackson (GJ) frame [4];
- the direction of the  $J/\psi$  in the center-of-mass system of the colliding hadrons (helicity frame, HX);
- the bisector between the directions of the beam momentum and of the opposite of the target momentum (as seen in the  $J/\psi$  rest frame) in the Collins-Soper (CS) frame [5].

The results of the present analysis are presented in all of these frames.

The values of  $\lambda_\theta$ ,  $\lambda_\phi$  and  $\lambda_{\theta\phi}$  are extracted from the data by considering single-variable projected angular distributions. When averaged over  $\phi$  and  $\cos\theta$ , respectively, the angular distribution of the decay leptons is reduced to the forms

$$\frac{dN}{d(\cos\theta)} \propto 1 + \lambda_\theta \cos^2\theta \quad (2)$$

<sup>1</sup> The sign of the measured  $\lambda_{\theta\phi}$  depends on the chosen orientation of the  $y$  axis (the one perpendicular to the plane of the colliding hadrons). In the convention adopted for the present analysis, the  $y$  axis is oriented as the vector product of the beam momentum and the target momentum,  $\mathbf{p}_{\text{beam}} \times \mathbf{p}_{\text{target}}$ .

and

$$\frac{dN}{d\phi} \propto 1 + \frac{2\lambda_\phi}{3 + \lambda_\theta} \cos(2\phi). \quad (3)$$

One possible way of determining the value of  $\lambda_{\theta\phi}$  is to define the variable  $\phi_\theta$  as

$$\phi_\theta = \begin{cases} \phi - \frac{3}{4}\pi & \text{for } \cos\theta < 0 \\ \phi - \frac{\pi}{4} & \text{for } \cos\theta > 0 \end{cases} \quad (4)$$

and measure the distribution

$$\frac{dN}{d\phi_\theta} \propto 1 + \frac{\sqrt{2}\lambda_{\theta\phi}}{3 + \lambda_\theta} \cos\phi_\theta. \quad (5)$$

## 3 Results

The efficiency-corrected single-variable angular distributions averaged over the accepted phase space ( $-0.34 < x_F < 0.14$ ,  $0 < p_T < 5.4$  GeV/ $c$ ) are shown in Fig. 1 with statistical uncertainties only. The results are given separately in the two decay channels ( $\mu^+\mu^-$ ,  $e^+e^-$ ) for carbon and tungsten target data combined. As can be seen, the measured distributions follow the correct symmetric and/or periodic behaviour expressed by the formulas in Eqs. 2, 3 and 5, indicating a good level of reliability of the acceptance and efficiency correction procedures; the chi-square probabilities obtained by fitting the distributions are on average 15% and 50% in the muon and electron channels, respectively. The values of the output parameters of the fits are listed in Table 1. The difference between the values measured in the two channels is always less than  $1.3\sigma$ . All results presented hereafter are averages of muon and electron measurements. We remark that a preliminary value of  $-0.35 \pm 0.04$  was used for the effective  $\lambda_\theta$  (CS frame) in the evaluation of systematic uncertainties of a previous HERA-B analysis [2]; such value deviates slightly, but well within errors, from the combined value in Table 1.

The final results including the estimated systematic uncertainties are displayed in Fig. 2 as a function of the transverse momentum and Feynman- $x$  of the  $J/\psi$ . As before, the two target data samples have been combined. The corresponding numerical values are listed in Tables 2, 3 and 4, where  $\langle p_T \rangle$  and  $\langle x_F \rangle$  indicate averages over the  $J/\psi$ 's reconstructed in a given bin. The bin boundaries are defined by the following lists: 0, 0.5, 1.0, 1.5, 2.5, 5.4 GeV/ $c$  (0, 0.2, 0.4, 0.6, 0.8, 1.0, 1.5, 2.5, 5.4 GeV/ $c$  for the helicity frame) for  $p_T$  and  $-0.34, -0.15, -0.10, -0.05, 0, 0.05, 0.14$  for  $x_F$ . The systematic errors have been evaluated with the procedure already described in our report on the measurement of the  $J/\psi$  kinematic distributions [3], taking into account the impact of signal selection and optimization, signal counting method, differences in acquisition conditions, and the kinematics of the MC generation. Additional systematic tests consisted in fitting the angular distributions excluding the angular ranges with the lowest efficiency. Statistical and systematic errors are obviously correlated from frame to frame. The systematic errors in different  $p_T/x_F$  bins are partly correlated.

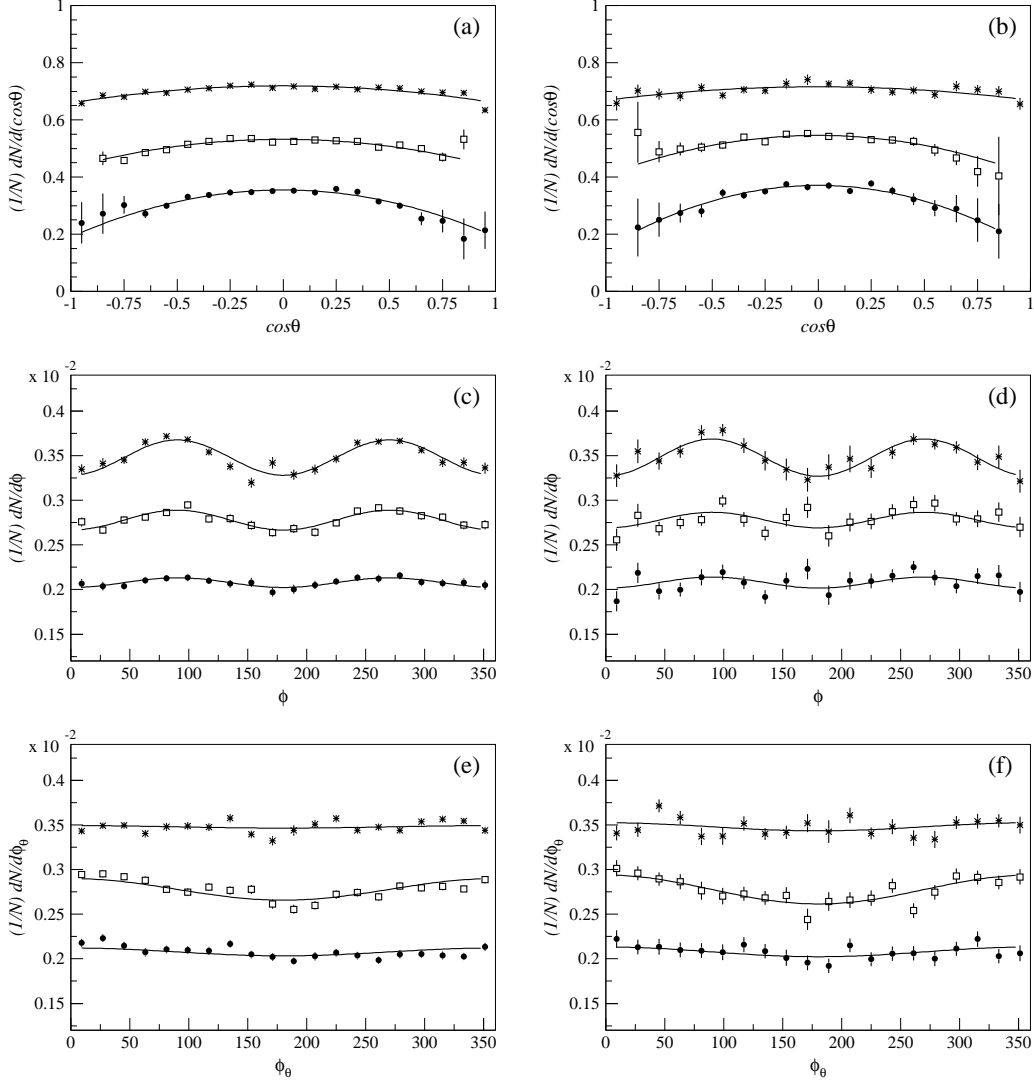


**Fig. 1.** Efficiency-corrected distributions of the angular variables  $\cos\theta$  (a, b),  $\phi$  (c, d) and  $\phi_\theta$  (e, f) measured in the muon (left column) and electron (right column) decay channels of the  $J/\psi$  over the whole visible phase space. The results obtained in the Collins-Soper, Gottfried-Jackson and helicity frames are represented, respectively, by black circles, white squares and asterisks. The errors are only statistical. For a better visualizations, the Collins-Soper and helicity distributions are displayed with their actual values shifted by a constant. The distributions are fitted with the curves of Eqs. 2, 3 and 5.

**Table 1.** Output parameters obtained by fitting the distributions shown in Fig. 1 with the curves of Eqs. 2, 3 and 5. The errors in the parameters reflect only statistical uncertainties of the distributions. The errors are correlated from one frame to another. The systematic uncertainties for the average values are in all frames of the order of 0.05 for  $\lambda_\theta$ , 0.02 for  $\lambda_\phi$  and 0.015 for  $\lambda_{\theta\phi}$ .

| Frame/channel    | $\lambda_\theta$   | $\lambda_\phi$       | $\lambda_{\theta\phi}$ |
|------------------|--------------------|----------------------|------------------------|
| CS/ $\mu^+\mu^-$ | $-0.296 \pm 0.029$ | $-0.0194 \pm 0.0051$ | $0.0158 \pm 0.0049$    |
| CS/ $e^+e^-$     | $-0.383 \pm 0.061$ | $-0.022 \pm 0.011$   | $0.0195 \pm 0.0096$    |
| CS/avg.          | $-0.313 \pm 0.026$ | $-0.0199 \pm 0.0046$ | $0.0168 \pm 0.0043$    |
| GJ/ $\mu^+\mu^-$ | $-0.185 \pm 0.021$ | $-0.0400 \pm 0.0051$ | $0.0433 \pm 0.0051$    |
| GJ/ $e^+e^-$     | $-0.256 \pm 0.051$ | $-0.031 \pm 0.011$   | $0.058 \pm 0.010$      |
| GJ/avg.          | $-0.195 \pm 0.019$ | $-0.0385 \pm 0.0046$ | $0.0463 \pm 0.0045$    |
| HX/ $\mu^+\mu^-$ | $-0.115 \pm 0.012$ | $-0.0714 \pm 0.0055$ | $0.0049 \pm 0.0049$    |
| HX/ $e^+e^-$     | $-0.092 \pm 0.027$ | $-0.075 \pm 0.012$   | $0.0161 \pm 0.0094$    |
| HX/avg.          | $-0.111 \pm 0.011$ | $-0.0720 \pm 0.0050$ | $0.0073 \pm 0.0043$    |

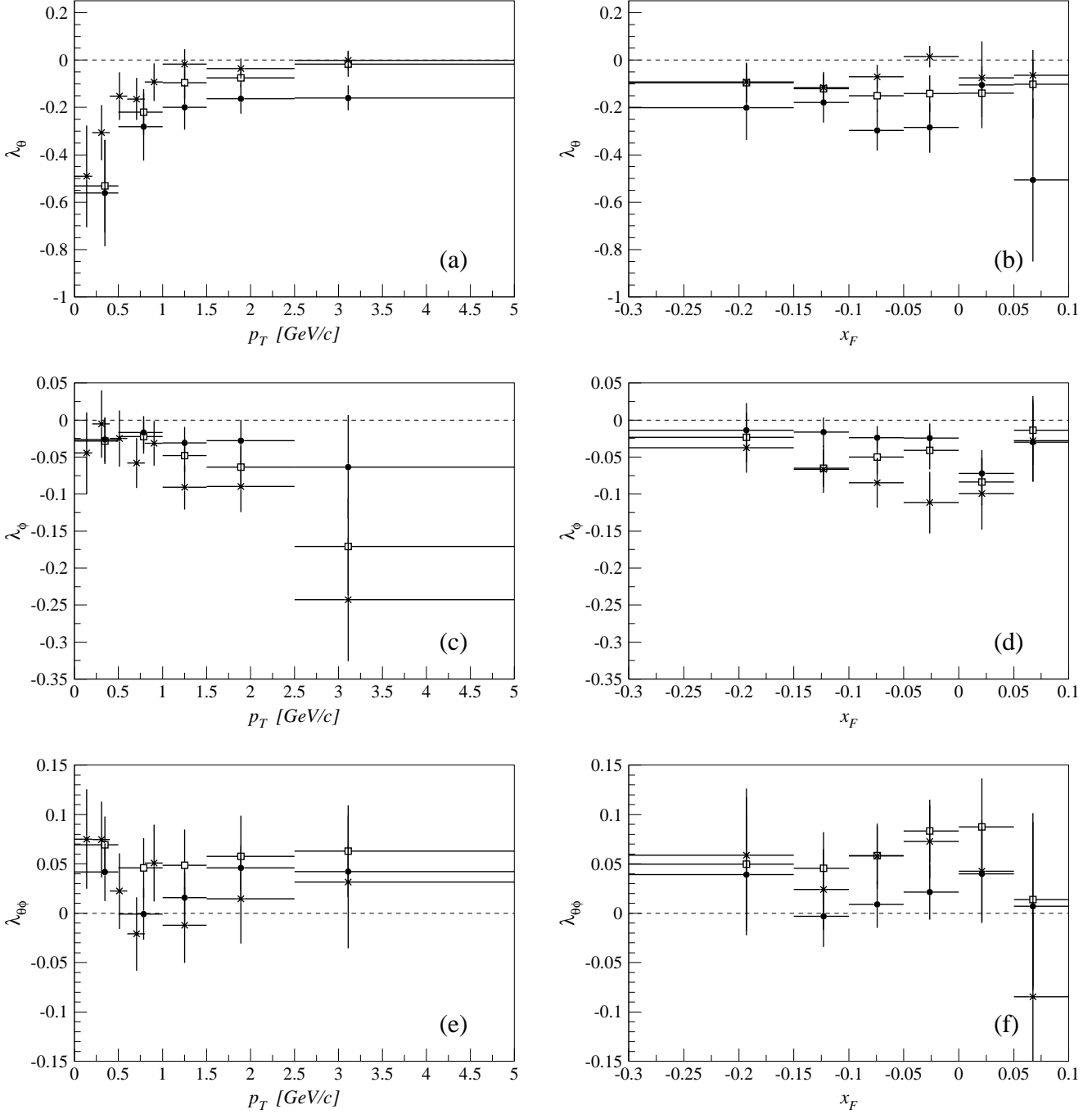


**Fig. 2.** The parameters  $\lambda_\theta$  (a, b),  $\lambda_\phi$  (c, d) and  $\lambda_{\theta\phi}$  (e, f) measured as functions of the average reconstructed  $p_T$  (left column) and  $x_F$  (right column). The results obtained in the Collins-Soper, Gottfried-Jackson and helicity frames are represented, respectively, by black circles, white squares and asterisks. The vertical errors bars represent quadratic sums of statistical and systematic uncertainties. The horizontal bars indicate the adopted binning.

The results indicate an anisotropy of the  $J/\psi$  decay angular distribution, visible in either its polar or azimuthal projections (in the CS and HX frames, respectively), or in both (GJ frame). Moreover, there is a definite hierarchy in the magnitudes of the parameters  $\lambda_\theta$  and  $\lambda_\phi$ . In particular, the polar anisotropy ( $\lambda_\theta < 0$ ) increases when going from the HX to the CS frame, while the azimuthal parameter  $\lambda_\phi$  changes following a reversed order. Both parameters have in-between magnitudes in the GJ frame. A kinematic dependence characterizes the results. For example, the magnitude of the polarization parameter  $\lambda_\theta$  increases with decreasing  $p_T$ . This low- $p_T$  effect is the same in the three frames – as expected from the fact that all frames coincide at  $p_T = 0$  – whereas different polarization magnitudes are measured at higher  $p_T$ , following the already mentioned hierarchy.

By performing a target-dependent analysis, generally small differences between the polarization parameters measured with carbon and tungsten data have been found and taken into account in the systematic errors of the already shown combined measurements. However, the results for the parameter  $\lambda_\theta$  show a slightly significant target dependence in the lowest  $p_T$  bin. The polarization measured in the CS frame as a function of  $p_T$  and  $x_F$  is shown in Fig. 3 for the two target materials; the numbers are listed in Table 5. In the first  $p_T$  bin, carbon and tungsten results differ by about  $3\sigma$  at the statistical level; the significance of the difference is reduced to the  $2\sigma$  level when also the systematic errors are included in the comparison.

Since the largest polarization effects are seen at low  $p_T$ , special attention has been devoted to the investigation of the systematic variations in the value of  $\lambda_\theta$  for  $0 < p_T < 0.5$  GeV/ $c$ . In fact, the determination of the low- $p_T$  efficiency is especially sensitive to the Monte Carlo description of the detector region close to the beam pipe. Various tests have been performed, which consisted in reducing the geometrical acceptance around the beam pipe, changing the beam direction in the Monte Carlo and testing different selection criteria for the low momentum leptons. As an extreme check, the acceptance determination has been varied to reproduce the detector conditions of acquisition periods not correlated to the considered sample. Final systematic uncertainties of  $\simeq 0.1$  and  $\simeq 0.2$  have been evaluated for  $\lambda_\theta$  for the carbon and tungsten targets, respectively (Table 5).

## 4 Conclusions

HERA-B has measured the two-lepton decay angular distribution of  $J/\psi$ 's produced inclusively in proton-nucleus collisions, using the decay channels  $e^+e^-$  and  $\mu^+\mu^-$ . The distributions of the polar and azimuthal angles have been determined in three different polarization frames. The results can be summarized as follows.

- In the observed phase space,  $\lambda_\theta$  is negative, indicating that the  $J/\psi$ 's are produced with a preferred spin component 0 along the reference axis.

- There is a definite hierarchy for the values of the decay angular parameters measured in different frames: the polar and azimuthal parameters satisfy the relations

$$\begin{aligned} |\lambda_\theta(\text{HX})| &< |\lambda_\theta(\text{GJ})| < |\lambda_\theta(\text{CS})| \\ |\lambda_\phi(\text{HX})| &> |\lambda_\phi(\text{GJ})| > |\lambda_\phi(\text{CS})|, \end{aligned}$$

while  $\lambda_{\theta\phi}$  is significantly different from zero only in the GJ frame.

- The polarization effects depend on the kinematics of the  $J/\psi$ . In particular, the polar anisotropy increases with decreasing  $p_T$  and is maximal in the limit  $p_T \rightarrow 0$ .

The different results obtained in the three frames – in terms of both polar and azimuthal distributions – are an example which shows that an analysis limited to only one frame and one polarization parameter is in general incomplete. For example, the present measurement of only the polarization parameter  $\lambda_\theta$  (i.e. ignoring  $\lambda_\phi$ ) in the HX frame for  $p_T > 1$  GeV/ $c$  may be misunderstood as a significant indication of unpolarized  $J/\psi$  production.

Among existing measurements of the parameter  $\lambda_\theta$ , E866 [6] (p-Cu at  $\sqrt{s} = 38.8$  GeV) has measured in the CS frame a  $p_T$ -independent polarization consistent with zero, while the CDF Run II [7] data ( $p\bar{p}$  at  $\sqrt{s} = 1.96$  TeV) indicate a negative polarization in the HX frame increasing in magnitude with increasing  $p_T$ . These results have been obtained in kinematic ranges (E866:  $x_F > 0.25$ , CDF:  $p_T > 5$  GeV/ $c$ ) which have no overlap with the HERA-B data and between each other. The three results are therefore not in contradiction; their comparison has to be interpreted as a further indication that the observed polarization effects change with varying kinematic conditions of the produced  $J/\psi$ .

## Acknowledgments

We express our gratitude to the DESY laboratory for the strong support in setting up and running the HERA-B experiment. We are also indebted to the DESY accelerator group for their continuous efforts to provide good and stable beam conditions. The HERA-B experiment would not have been possible without the enormous effort and commitment of our technical and administrative staff. It is a pleasure to thank all of them.

## References

1. I. Abt *et al.* (HERA-B Collaboration), Eur. Phys. J. **C49** (2007) 545.
2. I. Abt *et al.* (HERA-B Collaboration), submitted to Phys. Rev. D, arXiv:0807.2167v1.
3. I. Abt *et al.* (HERA-B Collaboration), DESY-08-180, arXiv:0812.0734v1 [hep-ex].
4. K. Gottfried and J.D. Jackson, Il Nuovo Cimento, **33** (1964) 309.
5. J.C. Collins and D.E. Soper, Phys. Rev. **D16** (1977) 2219.
6. T.H. Chang *et al.* (E866 Collaboration), Phys. Rev. Lett. **91** (2003) 211801.
7. A. Abulencia *et al.* (CDF Collaboration), Phys. Rev. Lett. **99** (2007) 132001.

**Table 2.** Values of the parameters  $\lambda_\theta$ ,  $\lambda_\phi$  and  $\lambda_{\theta\phi}$  measured in the Collins-Soper frame as functions of the average reconstructed  $p_T$  and  $x_F$  for combined carbon and tungsten data. The errors are statistical and systematic.

| $\langle p_T \rangle$ (GeV/c) | $\lambda_\theta$             | $\lambda_\phi$               | $\lambda_{\theta\phi}$       |
|-------------------------------|------------------------------|------------------------------|------------------------------|
| 0.35                          | $-0.56 \pm 0.07 \pm 0.21$    | $-0.026 \pm 0.013 \pm 0.027$ | $0.042 \pm 0.020 \pm 0.022$  |
| 0.79                          | $-0.28 \pm 0.05 \pm 0.13$    | $-0.017 \pm 0.010 \pm 0.020$ | $-0.001 \pm 0.014 \pm 0.022$ |
| 1.25                          | $-0.199 \pm 0.046 \pm 0.083$ | $-0.031 \pm 0.012 \pm 0.018$ | $0.016 \pm 0.014 \pm 0.021$  |
| 1.89                          | $-0.164 \pm 0.049 \pm 0.039$ | $-0.028 \pm 0.017 \pm 0.023$ | $0.046 \pm 0.015 \pm 0.017$  |
| 3.11                          | $-0.159 \pm 0.040 \pm 0.034$ | $-0.063 \pm 0.035 \pm 0.061$ | $0.042 \pm 0.024 \pm 0.011$  |
| $\langle x_F \rangle$         | $\lambda_\theta$             | $\lambda_\phi$               | $\lambda_{\theta\phi}$       |
| -0.193                        | $-0.202 \pm 0.072 \pm 0.116$ | $-0.014 \pm 0.019 \pm 0.032$ | $0.039 \pm 0.023 \pm 0.057$  |
| -0.123                        | $-0.179 \pm 0.050 \pm 0.068$ | $-0.017 \pm 0.014 \pm 0.014$ | $-0.003 \pm 0.019 \pm 0.024$ |
| -0.074                        | $-0.296 \pm 0.052 \pm 0.068$ | $-0.024 \pm 0.010 \pm 0.012$ | $0.009 \pm 0.016 \pm 0.018$  |
| -0.026                        | $-0.284 \pm 0.051 \pm 0.094$ | $-0.025 \pm 0.011 \pm 0.017$ | $0.021 \pm 0.013 \pm 0.025$  |
| 0.021                         | $-0.10 \pm 0.11 \pm 0.15$    | $-0.072 \pm 0.013 \pm 0.029$ | $0.040 \pm 0.018 \pm 0.044$  |
| 0.067                         | $-0.51 \pm 0.27 \pm 0.22$    | $-0.030 \pm 0.025 \pm 0.047$ | $0.007 \pm 0.039 \pm 0.076$  |

**Table 3.** Values of the parameters  $\lambda_\theta$ ,  $\lambda_\phi$  and  $\lambda_{\theta\phi}$  measured in the Gottfried-Jackson frame as functions of the average reconstructed  $p_T$  and  $x_F$  for combined carbon and tungsten data. The errors are statistical and systematic.

| $\langle p_T \rangle$ (GeV/c) | $\lambda_\theta$             | $\lambda_\phi$               | $\lambda_{\theta\phi}$      |
|-------------------------------|------------------------------|------------------------------|-----------------------------|
| 0.35                          | $-0.53 \pm 0.06 \pm 0.19$    | $-0.029 \pm 0.014 \pm 0.028$ | $0.069 \pm 0.020 \pm 0.020$ |
| 0.79                          | $-0.219 \pm 0.033 \pm 0.091$ | $-0.022 \pm 0.010 \pm 0.021$ | $0.046 \pm 0.014 \pm 0.027$ |
| 1.25                          | $-0.096 \pm 0.033 \pm 0.059$ | $-0.048 \pm 0.014 \pm 0.018$ | $0.049 \pm 0.017 \pm 0.032$ |
| 1.89                          | $-0.075 \pm 0.025 \pm 0.031$ | $-0.064 \pm 0.017 \pm 0.022$ | $0.058 \pm 0.018 \pm 0.037$ |
| 3.11                          | $-0.018 \pm 0.041 \pm 0.033$ | $-0.171 \pm 0.036 \pm 0.054$ | $0.063 \pm 0.026 \pm 0.038$ |
| $\langle x_F \rangle$         | $\lambda_\theta$             | $\lambda_\phi$               | $\lambda_{\theta\phi}$      |
| -0.193                        | $-0.096 \pm 0.039 \pm 0.075$ | $-0.023 \pm 0.021 \pm 0.026$ | $0.050 \pm 0.024 \pm 0.063$ |
| -0.123                        | $-0.120 \pm 0.033 \pm 0.063$ | $-0.065 \pm 0.015 \pm 0.020$ | $0.046 \pm 0.020 \pm 0.031$ |
| -0.074                        | $-0.151 \pm 0.028 \pm 0.063$ | $-0.050 \pm 0.012 \pm 0.020$ | $0.059 \pm 0.018 \pm 0.024$ |
| -0.026                        | $-0.141 \pm 0.031 \pm 0.070$ | $-0.041 \pm 0.011 \pm 0.023$ | $0.083 \pm 0.014 \pm 0.029$ |
| 0.021                         | $-0.140 \pm 0.057 \pm 0.084$ | $-0.084 \pm 0.013 \pm 0.029$ | $0.088 \pm 0.019 \pm 0.045$ |
| 0.067                         | $-0.10 \pm 0.10 \pm 0.10$    | $-0.014 \pm 0.026 \pm 0.039$ | $0.014 \pm 0.049 \pm 0.072$ |

**Table 4.** Values of the parameters  $\lambda_\theta$ ,  $\lambda_\phi$  and  $\lambda_{\theta\phi}$  measured in the helicity frame as functions of the average reconstructed  $p_T$  and  $x_F$  for combined carbon and tungsten data. The errors are statistical and systematic.

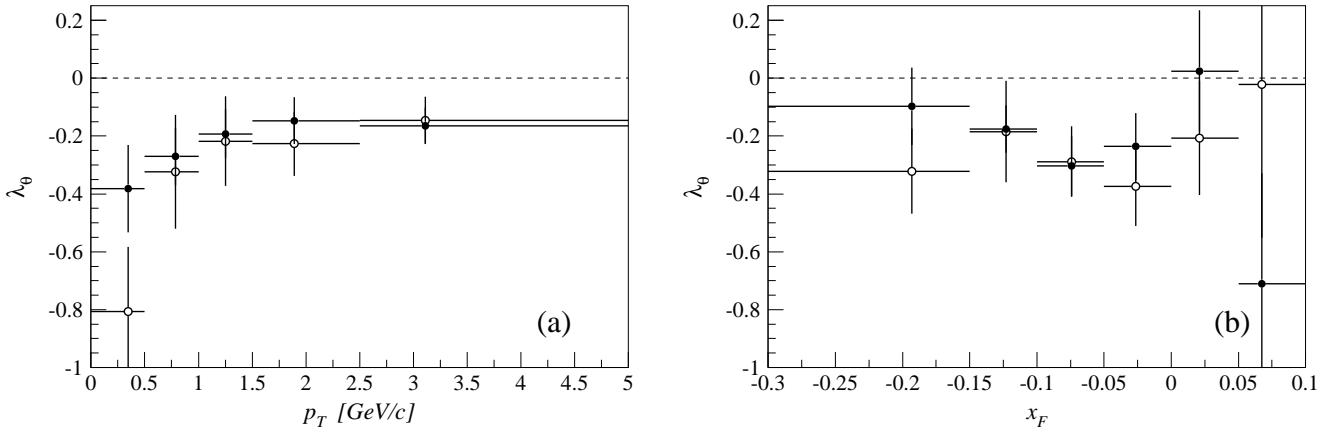
| $\langle p_T \rangle$ (GeV/c) | $\lambda_\theta$             | $\lambda_\phi$               | $\lambda_{\theta\phi}$       |
|-------------------------------|------------------------------|------------------------------|------------------------------|
| 0.14                          | $-0.49 \pm 0.07 \pm 0.20$    | $-0.045 \pm 0.029 \pm 0.047$ | $0.075 \pm 0.043 \pm 0.026$  |
| 0.31                          | $-0.31 \pm 0.05 \pm 0.11$    | $-0.005 \pm 0.021 \pm 0.041$ | $0.075 \pm 0.028 \pm 0.027$  |
| 0.51                          | $-0.153 \pm 0.031 \pm 0.096$ | $-0.025 \pm 0.017 \pm 0.034$ | $0.022 \pm 0.026 \pm 0.028$  |
| 0.71                          | $-0.164 \pm 0.026 \pm 0.085$ | $-0.058 \pm 0.018 \pm 0.029$ | $-0.021 \pm 0.023 \pm 0.030$ |
| 0.90                          | $-0.093 \pm 0.028 \pm 0.075$ | $-0.031 \pm 0.017 \pm 0.025$ | $0.051 \pm 0.023 \pm 0.031$  |
| 1.25                          | $-0.017 \pm 0.020 \pm 0.059$ | $-0.091 \pm 0.022 \pm 0.021$ | $-0.012 \pm 0.017 \pm 0.034$ |
| 1.89                          | $-0.037 \pm 0.021 \pm 0.037$ | $-0.090 \pm 0.026 \pm 0.023$ | $0.014 \pm 0.017 \pm 0.042$  |
| 3.11                          | $-0.001 \pm 0.037 \pm 0.016$ | $-0.243 \pm 0.055 \pm 0.063$ | $0.032 \pm 0.027 \pm 0.062$  |
| $\langle x_F \rangle$         | $\lambda_\theta$             | $\lambda_\phi$               | $\lambda_{\theta\phi}$       |
| -0.193                        | $-0.092 \pm 0.037 \pm 0.067$ | $-0.037 \pm 0.023 \pm 0.025$ | $0.059 \pm 0.025 \pm 0.062$  |
| -0.123                        | $-0.117 \pm 0.026 \pm 0.050$ | $-0.067 \pm 0.017 \pm 0.027$ | $0.024 \pm 0.021 \pm 0.035$  |
| -0.074                        | $-0.070 \pm 0.024 \pm 0.043$ | $-0.085 \pm 0.015 \pm 0.030$ | $0.058 \pm 0.016 \pm 0.029$  |
| -0.026                        | $0.014 \pm 0.019 \pm 0.041$  | $-0.112 \pm 0.023 \pm 0.034$ | $0.073 \pm 0.016 \pm 0.033$  |
| 0.021                         | $-0.075 \pm 0.023 \pm 0.043$ | $-0.100 \pm 0.027 \pm 0.040$ | $0.042 \pm 0.020 \pm 0.048$  |
| 0.067                         | $-0.064 \pm 0.041 \pm 0.049$ | $-0.028 \pm 0.029 \pm 0.047$ | $-0.085 \pm 0.044 \pm 0.073$ |

**Table 5.** Values of the parameter  $\lambda_\theta$  measured in the Collins-Soper frame as a function of the average reconstructed  $p_T$  and  $x_F$  for carbon (C) and tungsten (W) data. The errors are statistical and systematic.

| $\langle p_T \rangle$ (GeV/c) | $\lambda_\theta$ (C)         | $\lambda_\theta$ (W)         |
|-------------------------------|------------------------------|------------------------------|
| 0.35                          | $-0.38 \pm 0.10 \pm 0.11$    | $-0.81 \pm 0.10 \pm 0.20$    |
| 0.79                          | $-0.271 \pm 0.062 \pm 0.078$ | $-0.32 \pm 0.09 \pm 0.17$    |
| 1.25                          | $-0.192 \pm 0.054 \pm 0.066$ | $-0.22 \pm 0.09 \pm 0.13$    |
| 1.89                          | $-0.147 \pm 0.062 \pm 0.052$ | $-0.227 \pm 0.081 \pm 0.076$ |
| 3.11                          | $-0.164 \pm 0.049 \pm 0.039$ | $-0.146 \pm 0.072 \pm 0.038$ |

| $\langle x_F \rangle$ | $\lambda_\theta$ (C)         | $\lambda_\theta$ (W)      |
|-----------------------|------------------------------|---------------------------|
| -0.193                | $-0.097 \pm 0.090 \pm 0.099$ | $-0.32 \pm 0.12 \pm 0.08$ |
| -0.123                | $-0.176 \pm 0.054 \pm 0.062$ | $-0.18 \pm 0.15 \pm 0.10$ |
| -0.074                | $-0.304 \pm 0.079 \pm 0.067$ | $-0.29 \pm 0.07 \pm 0.10$ |
| -0.026                | $-0.236 \pm 0.062 \pm 0.097$ | $-0.37 \pm 0.09 \pm 0.10$ |
| 0.021                 | $0.03 \pm 0.15 \pm 0.15$     | $-0.21 \pm 0.17 \pm 0.10$ |
| 0.067                 | $-0.71 \pm 0.31 \pm 0.23$    | $-0.02 \pm 0.52 \pm 0.10$ |



**Fig. 3.** The parameter  $\lambda_\theta$  measured in the Collins-Soper frame in carbon (black points) and tungsten (white points) as functions of the average reconstructed  $p_T$  (a) and  $x_F$  (b). The vertical error bars represent quadratic sums of statistical and systematic uncertainties. The horizontal bars indicate the adopted binning.